

## Modeling Fermi Level Effects in Atomistic Simulations

Zudian Qin and Scott T. Dunham

Department of Electrical Engineering, University of Washington,  
Seattle, WA 98195

### ABSTRACT

In this work, variations in electron potential are incorporated into a Kinetic Lattice Monte Carlo (KLMC) simulator and applied to dopant diffusion in silicon. To account for the effect of dopants, the charge redistribution induced by an external point charge immersed in an electron (hole) sea is solved numerically using the quantum perturbation method. The local carrier concentrations are then determined by summing contributions from all ionized dopant atoms and charged point defects, from which the Fermi level of the system is derived by the Boltzmann equation. KLMC simulations with incorporated Fermi level effects are demonstrated for charged point defect concentration as a function of Fermi level, coupled diffusion phenomenon and field effect on doping fluctuations.

### INTRODUCTION

Kinetic Lattice Monte Carlo (KLMC) simulations study diffusion/clustering of defects in silicon at a microscopic level [1,2]. Simulations are performed on a silicon (diamond) lattice structure with impurities and point defects mapped to lattice sites. The system evolves through transitions from one atomic configuration to the next, by virtue of point defect migration/reaction. The rates of these transitions are determined by the migration barriers combined with changes in system energy associated with transitions:

$$\nu = \nu_0 \exp\left(\frac{-E_m}{k_B T}\right) \exp\left(\frac{E_i - E_f}{2k_B T}\right), \quad (1)$$

where  $E_m$  is the unbiased migration barrier,  $E_i$  and  $E_f$  are the system energies before and after the transition, and  $T$  is the system temperature. The system energies are calculated based on the atomic scale arrangement of impurities/defects, with parameters from *ab-initio* calculations and/or experimental observations. At each simulation step, one transition is chosen from the possible set based on the relative rates, and the system time is advanced by the inverse of the sum of the rates [1]. By only considering transitions (and not lattice vibrations) associated with defects and impurities present in the system, the KLMC method overcomes the time-scale limits associated with molecular dynamics to consider macroscopic systems and processing time scales.

The Fermi level is of critical importance in modeling dopant diffusion in silicon, but typically has not been included in atomistic simulations. Its importance manifests in two ways [3]: (i) charged point defect concentrations vary spatially with potential, and (ii) ionized dopant atoms as well as charged point defects experience electric fields due to spatial variations in the potential. Both effects are properly modeled in continuous simulations through the quantity of local carrier concentration, which is normally calculated from dopant profiles using the charge

neutrality assumption. Unfortunately, dopant concentration is no longer a valid concept at the atomic scale, where dopant atoms are considered to be discrete and point-like. To obtain local carrier concentrations, it is necessary to solve the Poisson equation in the presence of discrete point charges. In the following sections, we first present such a solution and show how a simple analytic form can model it. Then we demonstrate examples of KLMC simulations including potential variations.

## THEORY

To clearly define the problem, we consider a system with a defined uniform background carrier (electron or hole) concentration. To maintain charge neutrality in the region, an equal, but opposite dopant (donor or acceptor) concentration is also assumed. A pair of charges is then introduced into the system with the positive (negative) charge held at the origin (point-like) and the other mobile, negative (positive) charge released in the system. The challenge is then to solve the redistribution of the mobile charges in the neighborhood of the point charge at the origin under consideration of the background carrier screening.

We began with a classical solution to the problem, best known in its potential form as the screened Coulomb potential. The classical approach applies Boltzmann statistics and assumes the validity of linearization of the Boltzmann equation [4]. The solved charge distribution has the same form as the screened Coulomb potential:

$$\rho(\vec{r}) = \frac{-e}{4\pi L_D^2 r} \exp\left(\frac{-r}{L_D}\right), \quad (2)$$

where  $L_D$  is the Debye Length

$$L_D = \sqrt{\frac{k_{Si} \epsilon_0 (k_B T/e)}{e(n+p)}}. \quad (3)$$

Here,  $n$  and  $p$  are the background carrier concentrations. This solution has a simple analytic form, but diverges as  $r$  approaches zero, which is physically incorrect and causes a problem in the carrier concentrations derivation. To overcome this characteristic of the classical solution, a quantum approach is necessary.

In order to solve the problem in a practical way, two assumptions are made. The first assumption regards the system. We assume that the conduction band has a parabolic shape near its minima and conduction electrons are free. The second assumption is made on the approach, where we assume the quantum perturbation method is applicable to this problem.

Based on the two above assumptions, the generalized susceptibility of the system, characterizing the system's response to an external sinusoidal perturbation can be calculated as a function of spatial frequency [5]:

$$\chi(\vec{q}) = -\frac{6m^*}{\pi^3 \hbar^2} \int_0^\infty \frac{f(E_{\vec{k}})}{2\vec{k} \cdot \vec{q} + q^2} d^3 \vec{k}, \quad (4)$$

where  $q$  represents the spatial frequency of the sinusoidal perturbation,  $m^*$  is the effective mass of electrons ( $0.33m_e$ ), and the factor of six accounts for multiple band minima. The background carrier concentrations and system temperature enter as parameters through  $f(E_k)$ , the Fermi-Dirac distribution function, with the Fermi energy chosen to match the background carrier concentrations.

Given the susceptibility function of the system from Eq. (4), the induced charge distribution is calculated in response to an external point charge, which is represented by its Fourier components [5]:

$$\rho(\vec{r}) = -e \int_0^\infty \left[ \frac{k_{si}}{\varepsilon(\vec{q})} - 1 \right] \exp(i\vec{q} \cdot \vec{r}) \frac{d^3\vec{q}}{(2\pi)^3}, \quad (5)$$

where  $\varepsilon(\vec{q})$  is the dielectric function of the system

$$\varepsilon(\vec{q}) = k_{si} - \frac{e^2}{\varepsilon_0 q^2} \chi(\vec{q}). \quad (6)$$

## RESULTS

Eq. (5) was evaluated numerically and the results are shown in Figs. 1 and 2. Fig. 1 shows results for three distinct background carrier concentrations:  $5 \times 10^{18}$ ,  $1 \times 10^{19}$  and  $5 \times 10^{19} \text{ cm}^{-3}$ . Clearly, the charge distribution drops off more rapidly with an increasing background carrier concentration, indicating a stronger screening effect. Fig. 2 shows results for three different system temperatures of  $800^\circ\text{C}$ ,  $900^\circ\text{C}$  and  $1000^\circ\text{C}$ . As seen, there is only a weak dependence on temperature within the process temperature regime.

Upon examination of numerical results for different background carrier concentrations and temperatures, we find that the quantum solution can be modeled by:

$$\rho(r) = \rho(0) \frac{r_0}{\sqrt{r^2 + r_0^2}} \exp(-r/L_D), \quad (7)$$

where  $\rho(0)$  is the charge density at the origin, and  $r_0$  is a parameter representing best fitting to the numerical results. In fact,  $r_0$  is only a weak function of the background carrier concentration and temperature, and is approximately 0.8 nm. In Fig. 3, both the classical and quantum solutions are plotted, along with Eq. (7), which shows excellent agreement with the quantum solution over the entire range. The quantum solution matches the classical solution at long range, but deviates from it in the short range. Most significantly, it gives a finite value at the origin, where the classical solution diverges. Calculations are carried out over background carrier concentrations up to  $3 \times 10^{20} \text{ cm}^{-3}$ . Beyond this concentration limit, Friedel oscillations [5] appear and Eq. (7) no longer accurately predicts the numerical results.

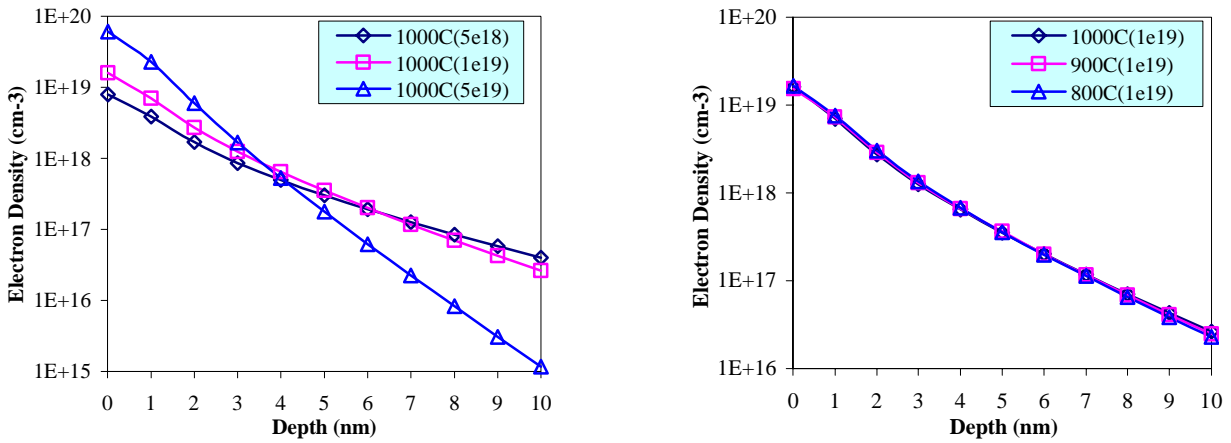


**Figure 1. (left side)** Electron distribution in the neighborhood of a positive point charge, calculated using quantum perturbation method for three distinct background carrier (electron) concentrations of  $5 \times 10^{18}$ ,  $1 \times 10^{19}$  and  $5 \times 10^{19}$  cm<sup>-3</sup> at temperature of 1000°C. As the background carrier concentration increases, the distribution profile drops off more rapidly due to stronger mobile carriers screening.

**Figure 2. (right side)** Electron distribution in the neighborhood of a positive point charge, calculated using quantum perturbation method for three different system temperatures of 1000°C, 900°C and 800°C with the background carrier (electron) concentration set to be  $1 \times 10^{19}$  cm<sup>-3</sup>. Distribution profiles show only a weak dependence on temperature.

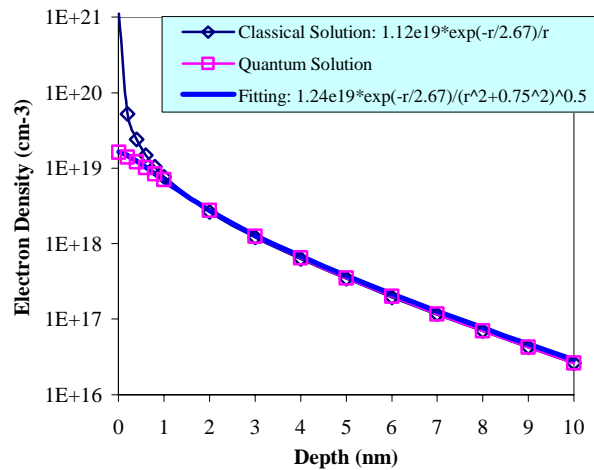


**Figure 3.** Electron distribution in the neighborhood of a positive point charge from both the classical and quantum solutions for a system with a background carrier (electron) concentration of  $1 \times 10^{19}$  cm<sup>-3</sup> and a temperature of 1000°C. The classical Debye length in this case is 2.67 nm. The quantum solution matches the classical solution at long range. Also plotted is the fitted curve  $1.24 \times 10^{19} \exp(-r/2.67)/(r^2+0.75^2)^{0.5}$ , which shows excellent agreement with the quantum solution over the entire range.

Given the charge distribution in the neighborhood of a single point charge, the local carrier concentrations can be, to first approximation, determined by summing contributions from all

ionized dopant atoms and charged defects, with a positive point charge (e.g., an ionized donor) inducing an electron cloud in its neighboring region and a negative charge (e.g., an ionized acceptor) inducing a hole cloud. The Fermi level is then derived from local carrier concentrations by the Boltzmann equation, as is usually done in continuum modeling. In the following section, we show example KLMC simulations with incorporated Fermi level effects.

## KLMC SIMULATIONS

As a first test, the charged defect concentration is characterized as a function of the local Fermi level. A negatively charged vacancy,  $V^-$ , is put in a box with a non-uniform background Arsenic (As) doping. We then measure the time that the vacancy spends at various locations, the residence time. As seen from Fig. 4, the residence time follows the background carrier concentration curve, as would be predicted by a continuum model.

Multiple dopants diffusing simultaneously interact via field effects. The next simulation illustrates this phenomenon. Initially, there is a uniform background Boron (B) and non-uniform As doping in the system. After the simulation, B is swept out of the junction region where the field gradient is the strongest, as seen in Fig. 5.

Channel dopant fluctuations are a concern for nanoscale devices as they impact transistor characteristics such as threshold voltage. The final simulation shows the effect of fields on dopant location fluctuation. Dopant atoms are first randomly initialized and the Fermi level at various locations is recorded. The diffusion is then performed and the Fermi level again recorded. Fig. 6 compares the results from these two calculations in terms of the Fermi level distribution in the system. The curves clearly show that the system has a more uniform potential after the diffusion, indicating a more uniform dopant distribution as a result of dopant/dopant repulsion, with the standard deviation in electrical potential dropping from 0.014 to 0.012eV.

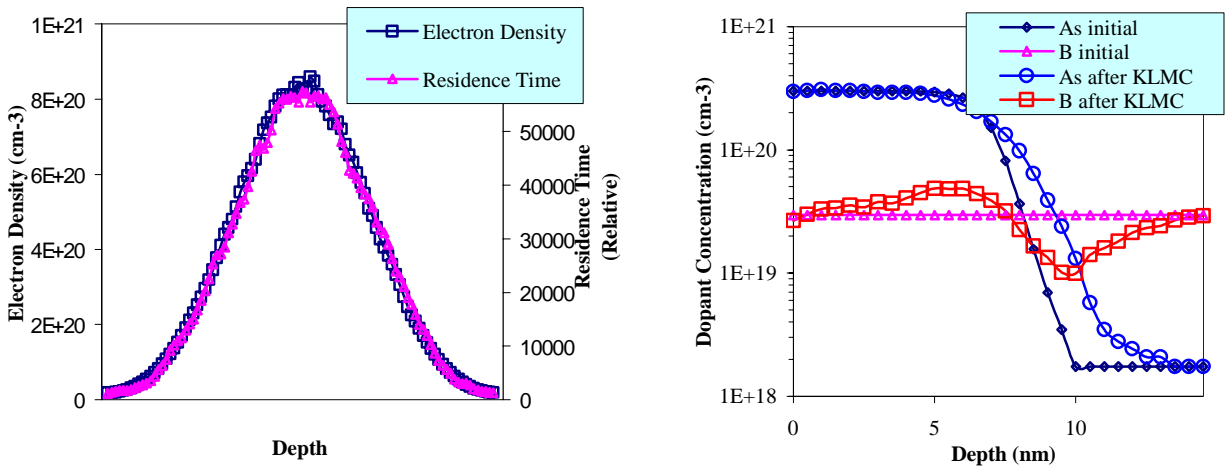


**Figure 4. (left side)** KLMC simulation shows residence time of a negatively charged vacancy at various locations matches background carrier concentration as predicted by a continuum model. **Figure 5. (right side)** KLMC simulation shows coupled diffusion due to field effects. B is swept out of the junction region by the present strong electric field.

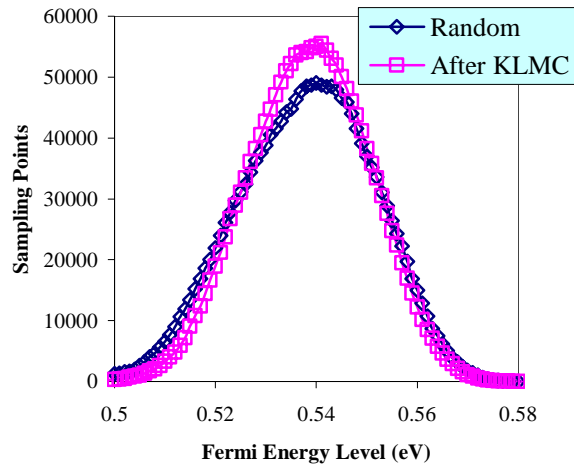


**Figure 6.** Results of KLMC simulation showing field effect on dopant location fluctuations. Plotted are Fermi level distributions in the system before and after diffusion simulation. The system has a narrowed field distribution after diffusion, indicating effect of dopant/dopant repulsion on dopant redistribution. Calculation gives a standard deviation of 0.12eV for the profile after diffusion, in contrast to 0.14eV for the initial (random) profile.

## CONCLUSIONS

We have solved the charge distribution in the neighborhood of a point charge using the quantum perturbation method and have shown that the solution can be expressed as a simple analytic function. KLMC simulations with this model incorporated gave expected results for charged defect concentration as a function of the Fermi level, illustrated coupled diffusion phenomenon and showed reduced channel dopant location fluctuation due to like-dopant repulsion.

## ACKNOWLEDGEMENT

This work was supported by the Semiconductor Research Corporation.

## REFERENCES

1. S. T. Dunham and C. D. Wu, *J. Appl. Phys.* **78**, 2362 (1995).
2. M. M. Bunea and S. T. Dunham, in *Semiconductor Process and Device Performance Modeling*, edited by S. T. Dunham and J. Nelson, (Mater. Res. Soc. Proc. **490**, Pittsburgh, PA, 1998) pp. 3-8.
3. P. M. Fahey, P. B. Griffin and J. D. Plummer, *Rev. Mod. Phys.* **61**, 289 (1989).
4. N. W. Ashcroft and N. D. Mermin, *Solid State Physics*, 1<sup>st</sup> ed. (Holt, Rinehart and Wilson, 1976) pp. 342.
5. J. Chazalviel, *Coulomb Screening by Mobile Charges: Applications to Materials Science, Chemistry, and Biology*, (Birkhäuser, 1998) pp. 27-34.